Accepted Manuscript

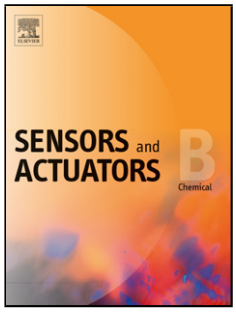

Title: SnO_2-MOF-Fabry-Perot optical sensor for relative humidity measurements

Authors: A. Lopez Aldaba, D. Lopez-Torres, C. Elosua, J.-L. Auguste, R. Jamier, P. Roy, F.J. Arregui, M. Lopez-Amo

PII: S0925-4005(17)32063-4
DOI: https://doi.org/10.1016/j.snb.2017.10.149
Reference: SNB 23453

To appear in: *Sensors and Actuators B*

Received date: 5-7-2017
Revised date: 3-10-2017
Accepted date: 25-10-2017

Please cite this article as: A.Lopez Aldaba, D.Lopez-Torres, C.Elosua, J.-L.Auguste, R.Jamier, P.Roy, F.J.Arregui, M.Lopez-Amo, SnO2-MOF-Fabry-Perot optical sensor for relative humidity measurements, Sensors and Actuators B: Chemical https://doi.org/10.1016/j.snb.2017.10.149

SnO_2-MOF-Fabry-Perot optical sensor for relative humidity measurements

A. Lopez Aldaba*[a], D. Lopez-Torres[a], C. Elosua[a], J.-L. Auguste[b], R. Jamier[b], P. Roy[b], F.J. Arregui[a] and M. Lopez-Amo[a]

[a]Universidad Pública de Navarra, Dept. of Electrical and Electronic Engineering, Institute of Smart Cities (ISC), and IDISNA, Campus Arrosadia, 31006, Pamplona, Spain.

[b]Xlim, Fibre Photonics Department, UMR CNRS/University of Limoges 7252, 123 Avenue Albert Thomas, 87060 Limoges Cedex, France

* aitor.lopez@unavara.es; phone +34 948 16 9841; fax +34948 16 9720

GRAPHICAL ABSTRACT

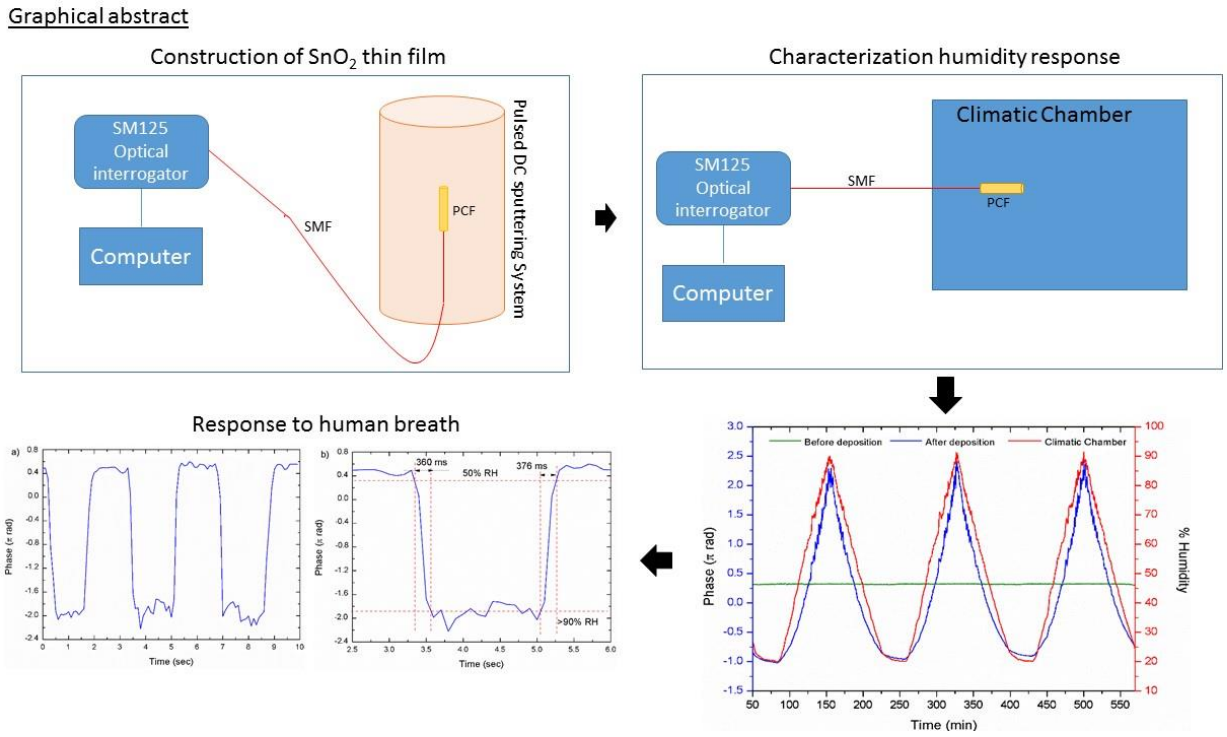

ABSTRACT

In this paper, a new optical fiber sensor for relative humidity measurements is presented and characterized. The sensor is based on a SnO_2 sputtering deposition on a microstructured optical fiber (MOF) low-finesse Fabry-Pérot (FP) sensing head. The feasibility of the device as a breathing sensor is also experimentally demonstrated. The interrogation of the sensing head is carried out by monitoring the Fast Fourier Transform phase variations of the FP interference frequency. This method substitutes the necessity of tracking the optical spectrum peaks or valleys, which can be a handicap when

noise or multiple contributions are present: therefore, it is low-sensitive to noise and to artifacts signal amplitude. The sensor shows a linear behavior in a wide relative humidity range (20%–90% relative humidity) in which the sensitivity is 0.14 rad/%; the maximum observed instability is 0.007 rad, whereas the highest hysteresis is 5% RH. The cross correlation with temperature is also considered and a method to lower its influence is proposed. For human breathing measurement, the registered rising and recovery times are 370 ms and 380 ms respectively.

Keywords: Photonic Crystal Fiber, Microstructured Optical Fiber, Fiber Sensor, Humidity Sensing, Breathe Sensing, Fast Fourier Transform.

1. Introduction

Optical fiber based sensors have shown great features to measure different parameters such as temperature, curvature, displacement, pressure, refractive index, electric field, relative humidity and gases, among others. Many types of optical fibers have been used for sensing along the time: standard silica based, plastic, doped, and photonic crystal fibers are some examples. Since the first experiments with microstructured optical fibers (MOFs), they have shown relevant improved characteristics compared to conventional optical fibers as well as a great potential for sensing applications, overcoming some of the standard optical fiber limitations [1]. Different geometries have been proposed for this kind of fibers. Among them, suspended-core MOFs present relatively large air holes surrounding a small core (typically a few microns diameter) that seems to be suspended along the fiber length but maintained by thin silica bridges. Distinct pure silica suspended-core fibers have been applied for instance in temperature and curvature sensing [4], gas sensing [5] or micro-displacement measurements [6].One of the most important type of MOF sensors are the ones based on evanescent field. These sensors have been used for different applications: simultaneous measurement of humidity and mechanical vibration [7], detection of biomolecules in aqueous solutions [8] as well as organic pollutants [9] or hydrogen detection [10] have been reported using such a kind of transducers.

Fiber based optical Fabry-Pérot (FP) interferometers are a common sensor configuration due to their compactness, simple configuration, design flexibility and dynamic range. A fiber based FP sensor is most of the times fabricated by splicing a section of a waveguide, which acts as cavity, to a standard optical fiber segment. This structure presents robustness and multiplexing capability. The FP cavity output signal consists of an interference pattern which is a function of the cavity length and of the refractive index of the cavity, or more precisely, the effective indices of the different modes supported by the fiber interferometer. FP cavities based on MOFs are also common structures. For instance, a hybrid structure that used a MOF as the guiding fiber, in combination with a hollow-core fiber and a single mode fiber (SMF), for high-temperature sensing, was demonstrated in [13]. Nitrogen sensors [14], chitosan based ones for relative humidity (RH) [15] as well as strain, temperature and pressure FP devices [16] have been also reported. Other fiber based sensors were implemented by fusing a small length of PCF to the end of a cleaved SMF for relative humidity ranged 40%-95% RH [18] or by chemical deposition of polymers [19].

Among optical fiber sensors, those based on nanocoatings have recently experienced a significant development [20]. Furthermore, new chemical deposition techniques, such as sputtering [21], allow the morphology of the deposited coatings to be controlled with high accuracy: as a consequence, the final features of the sensor (sensitivity, kinetics) are enhanced. SnO_2 depositions have shown great properties for sensing applications such as high sensitivity H_2S sensors [22], ethanol sensors [23], CO and NO_2 sensors [24] or smoke sensors [25]. There are several methods to prepare SnO_2 sensitive layers. To create a homogeneous layer on the surface of a pure silica optical fiber, sputtering depositions are commonly used [26].

Several relative humidity sensors using optical fiber substrates have already been reported: agarose gel layers on tapered fibers [29], hygroscopic layers on hetero-core based fibers [30], nano Fabry-Perot cavity sensors [31] and coatings on long-period and standard FBGs [32] are some remarkable examples. One of the most studied applications for the relative humidity sensors in the field of bio medical engineering is breathing monitoring. Fast response and recovery time are critical for this kind of measurements. Different types of breathing sensors have been experimentally reported: the most relevant ones are devices based on microstructured fiber [34], macrobending [35], medical textiles in which Bragg and time reflectometry sensors are embedded [36], devices based on nanostructured fibers [37] or plastic optical fiber (POF) [38].

A SnO_2 Fabry-Pérot interferometer implemented with a four-bridge dual highly coupled cores microstructured optical fiber is presented and characterized in this work. By monitoring the Fast Fourier Transform (FFT) phase variations of the FP interference frequency, an experimental study of this cavity's response towards relative humidity changes is described.

In a previous study, an initial characterization of the relative humidity sensor was performed by the FFT technique, showing the independence of the signal amplitude and avoiding the necessity of tracking the wavelength evolution in the spectrum, which makes the measurements more robust [39]. Furthermore, relevant factors such the optimization of sputtering thickness, an analysis of the response vs temperature variations, hysteresis error measurements, and a novel study though the optical backscatter reflectometer in order to observe the propagation of light and sputtering depth inside the MOF are studied in detail. Finally, an application for human breath monitoring on real time is proposed and validated.

2. Experimental

2.1 Microstructured optical fiber

A sample of a "four-bridge double-Y-shape-core MOF" was developed and fabricated using the stack and draw process. It presents four large air holes divided by four thin bridges (~800 nm), showing a suspended core of 6.5 µm by 806 nm and exhibiting a double Y shape, as can be seen in the SEM pictures shown in Fig. 1. This MOF presents multimodal and birefringence features [40]. Birefringence in the 1550 nm region was theoretically estimated in ~6.8×10^{-3} with a beat length of 350 µm.

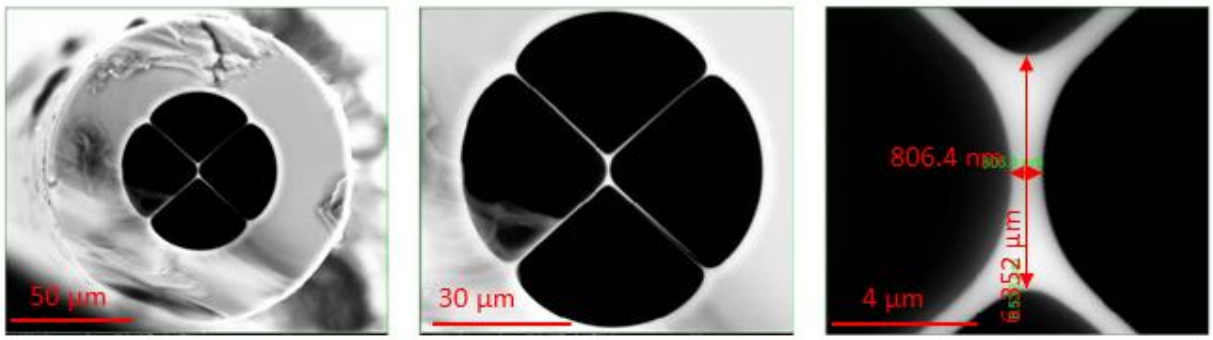

Fig. 1. Microscope photograph of the microstructured optical fiber (MOF)'s cross section.

This particular structure has interesting properties for gas sensing and chemical deposition processes: the presence of the four longitudinal air holes directly in contact with the fiber core allows the light guided in the core and the surrounding medium to interact directly through the evanescent field. Moreover, the reduced dimensions of the MOF core and the high numerical aperture (due to the effective refractive index difference between the core and air cladding) increases the evanescent field as it has been previously reported [41]. The air holes dimensions also allows different chemical compounds to be deposited, which leads to high sensitive layers.

2.2 Fabry-Perot cavity

The low-finesse Fabry-Pérot interferometer was fabricated by splicing a single mode fiber (Corning SMF-28) to ~700 µm of the four-bridge MOF, whose end was perpendicularly cleaved, as it is shown in Fig. 2. This delicate splice was made through a custom splice program due to the fragility of the MOF fiber, especially given by the bridge thickness. There is a trade-off between the cavity robustness and the MOF´s structural stability once the splicing arc is applied. The splice was made with a Fitel S175 fusion splicer with a custom developed program for this MOF and manual operation for its alignment. Results were obtained repeatedly as shown in [39, 40].

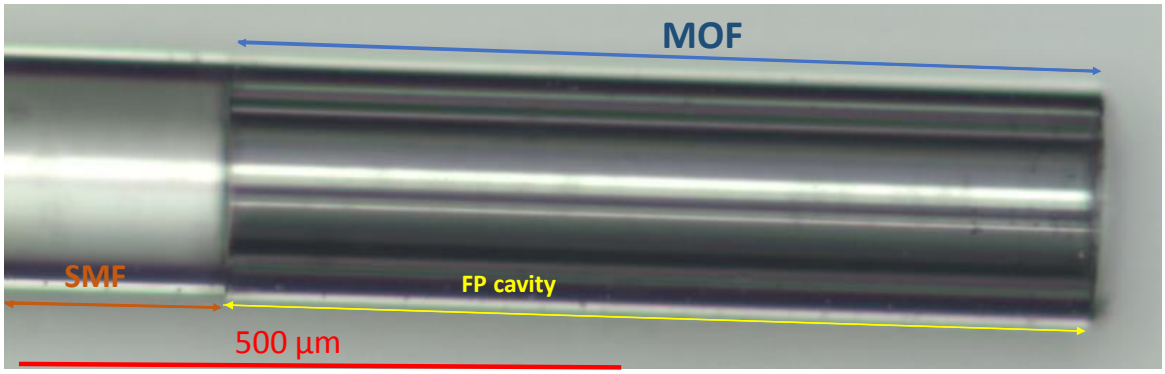

Fig. 2. Microscope photograph of the low-finesse Fabry-Pérot cavity.

By splicing a piece of MOF to a SMF, two low-reflectivity mirrors are formed at both ends of the MOF: one in the interface SMF-MOF due to the discontinuity in refractive index between both fibers; the other one is located at the interface MOF-air because this high discontinuity provides a Fresnel reflection (3.3%). Light is coupled from the SMF to the MOF, reflected at the MOF's end and then coupled back in the SMF. In this manner, a low-finesse Fabry-Pérot interferometer is created when a light beam reaches the cavity (MOF) and it is reflected several times between the two interfaces. Each beam has a certain phase difference with respect to the preceding one: this shift corresponds to the extra path length travelled inside the cavity. Due to the high loss of the MOF and the low reflectivity of the air-glass interface, high order reflections inside the cavity are neglected and therefore a low-finesse scenario is assumed which approximates a two-beam Fabry-Perot [43].

Assuming a two beam Fabry-Perot, the reflected signal obtained should follow equation (1), where $\Delta\lambda$ is the optical spectrum wavelength spacing, λ is the working wavelength, n is the refractive index and d is the MOF cavity length. Experimentally, λ = 1550 nm, d = 690 µm and n_{eff} = 1.37 [40].

$$\Delta\lambda = \frac{\lambda^2}{2nd} \qquad (1)$$

As a result, the experimental reflected spectrum is shown in Fig. 3.

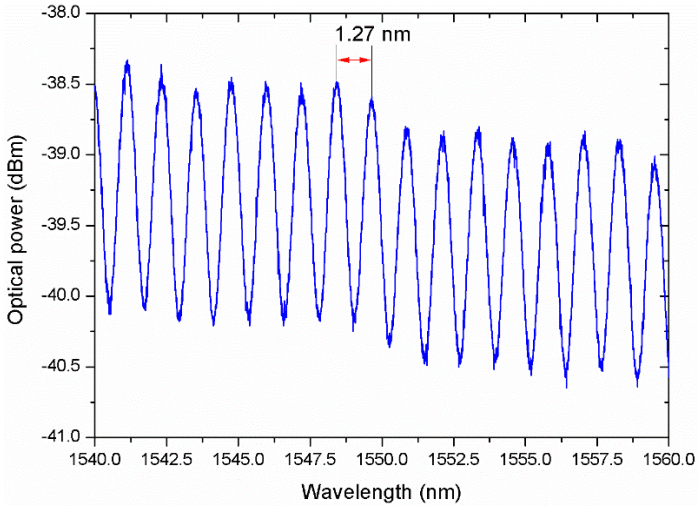

Fig. 3. Low-finesse FP reflected spectrum.

2.3 Experimental Setup

Fig. 4 presents the experimental set-up used to characterize the resulting sensor. Two commercial interrogating sensor devices were used to illuminate the sensing head and also to analyze the spectra of the signal guided back from the sensor. It should be noticed that in addition to their original purpose as FBG interrogators, this equipment can be used to interrogate other type if sensors in real time. The optical interrogators are remotely controlled by a MATLAB script which also computes the FFT real time analysis. The sensing head was placed into a climatic chamber where relative humidity ranges from 20% to 90% were applied at a constant temperature of 25ºC ± 1ºC to evaluate its response.

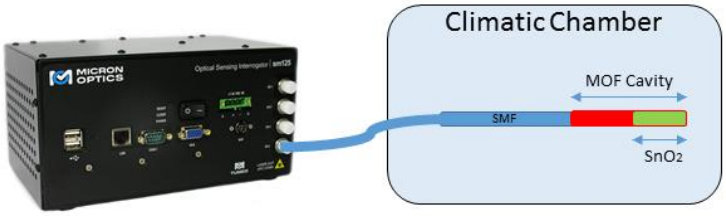

Fig. 4. Experimental setup for RH characterization.

Experimental measurements were carried out with two different optical interrogators showing dissimilar sample rates and spectral resolutions. A Micron Optics SM 125 optical sensing interrogator with a resolution of 5 pm and a maximum scan frequency of 1 Hz [44] was used to perform the characterization of the sensing head inside the climatic chamber (Angelantoni CH 250). For human breath measurements, higher sample rates were required, so that a Micron Optics si155 with a maximum sample rate of 1 kHz and 10 pm of resolution was employed. The sample rate was set to 10 Hz for breathing measurements.

A multi-LED light source (HP83437A) and Optical Spectrum Analyzer (OSA-HP86142A) combined with an optical circulator were used to monitor the interference pattern shift along the sputtering process as well as to test the sensor (as Fig. 5 illustrates).

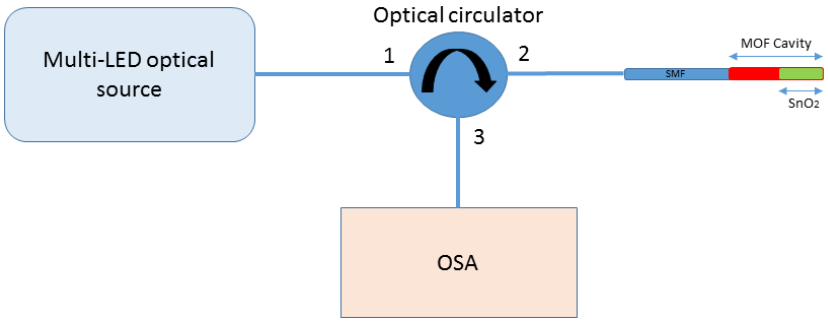

Fig. 5. Experimental setup for SnO_2 construction and breathe measurements.

Finally, to monitor the SnO_2 final deposition depth inside the MOF an Optical Backscatter Reflectometer (OBR 4600 Luna Technologies) with a spatial resolution of 10 µm was used in reflexive configuration (same as Fig. 4).

2.4 Sensing material

Several papers have shown very interesting results when tin dioxide (SnO_2) was deposited in different types of optical fibers to prepare relative humidity sensors [45]. Due to the structure of the MOF used in this work, SnO_2 can be deposited on the walls of the air holes of the short section of the MOF as well as on the top of the sensor head, which improves the sensitivity of previous devices. For this reason, the combination of MOF and SnO_2 is very interesting for sensing applications. The interaction between SnO_2 and H_2O molecules is due to the phenomena called physisorption by means of

the adsorption/desorption of these molecules [47]. The molecules of water interact just with the surface of the deposited film.

A SnO_2 (the sputtering target was purchased in ZhongNuo Advanced Material Techonology Co) thin film was deposited onto the low-finesse FP interferometer sensor head using a sputtering machine (Pulsed DC sputtering System, Nadetech Innovations). The sputtering process was performed with a partial pressure of Argon of $5x10^{-2}$ mb, a current of 160 mA and a voltage of 190 V. The distance between the sensor head and the SnO_2 target was set to 2 cm. Sputtering technique was selected because it is a reproducible process which allows a homogeneous thickness to be achieved, as it can be observed in the Fig.6. The nanofilm thickness is to be optimized because it is a critical parameter that determines the sensitivity of sensor.

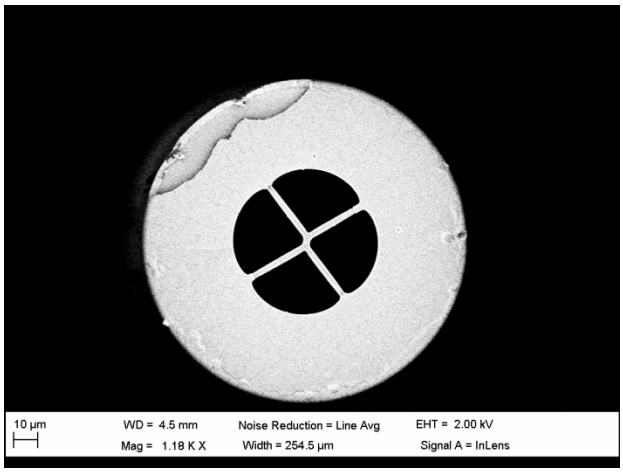

Fig. 6. Fiber cross section after deposition.

2.5 Optimization of the thin film thickness

In section 2.1, it has been mentioned that the presence of air holes in the fiber core allows a direct interaction between the light guided in the core and the surrounding medium through the evanescent field. Based on this explanation, when an optimal thickness of SnO_2 is sputtered on the walls of the MOF air holes, the interaction between the evanescent field of the guided light and the thin film is possible: it is the transduction mechanism, in which the thin film thickness is critical for the sensitivity. When the sensor is exposed to different relative humidity values, the refractive index of the surrounding medium changes shifting the interference pattern.

In order to achieve the optimal SnO_2 thin film that maximizes the sensitivity of the sensor, a 20 minutes long sputtering process was performed. Fig. 7 illustrates the evolution of the interference pattern peaks of the cavity during the sputtering process. The recorded shift depends on the deposition thickness and therefore the thin film effect can be studied by analyzing these data. In previous papers [48], it was found that the optimal point to stop the construction is when little thickness changes generate high wavelength shifts in the spectrum. In the current work, as it can be observed in Fig.7, when the thickness of the sensor is increased the wavelength shift of every peak is roughly the same and consequently, the slope of each of them is apparently the same. This is an important result of the sputtering process which means that the spectrum continues shifting during the whole deposition time but the sensitivity can be compromised. As [49] explains, if an unsuitable thickness is deposited onto the sensor, there are two different scenarios regarding to the sensor sensitivity: firstly, if the nanofilm thickness deposited is very thin, only a small part of the evanescent field interacts whit it; secondly, if the nanofilm thickness deposited is too high, the interaction between the evanescent field and the nanofilm that has adsorpted the eater molecules is not possible. In both of cases, the sensitivity of the sensor is not the optimal one.

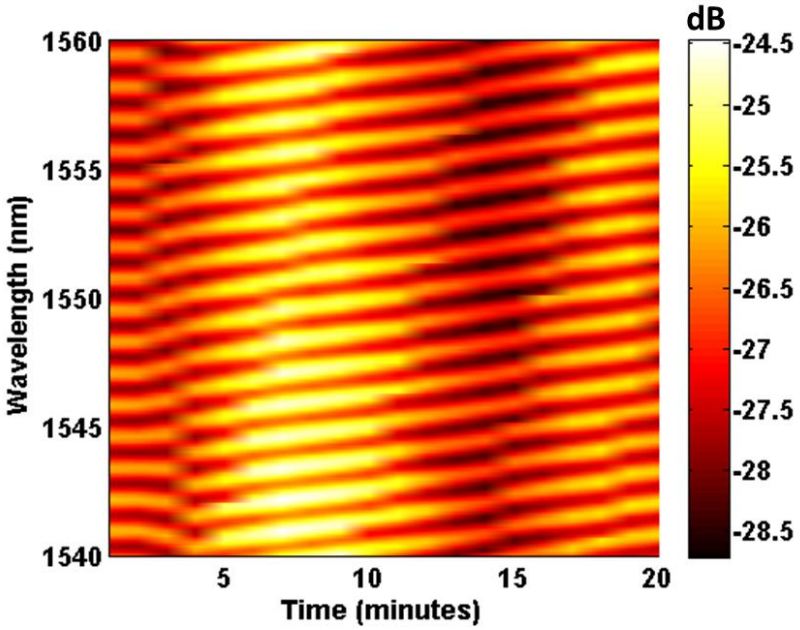

Fig. 7. Spectral (1540-1560 nm) evolution of the SnO_2 thin film MOF sensor transfer function during the sputtering process.

To analyze this problem and achieve the thin film thickness that optimizes the sensitivity of the sensor, five different devices were performed with distinct construction times. The times selected were 5', 7.5', 10', 12.5' and 15 minutes respectively. The sputtering time determines the thin film thickness and therefore the sensors' sensitivity as it can be seen in Fig.8. All the resulting sensors where tested within 20%-90% relative humidity ranges showing different sensitivities. Starting from a 5 minutes deposition, the sensitivity is gradually increased showing the best sensitivity at 10 minutes (0.014π rad/%, 0.018π rad/%, and 0.047π rad/% for 5', 7.5' and 10' respectively). Beyond 10 minutes, the SnO_2 thin film becomes thicker than the evanescent field penetration and consequently, the sensitivity decreases (0.023π rad/% and 0.02π rad/% for 12.5' and 15' respectively). The thickness for each case was estimated by comparing SEM images of the sensing head's cross section before and after deposition (Fig.1 and Fig. 4 respectively). The 10 minutes deposited sensor presents a thin film thickness of 1.10 µm ± 0.09 µm.

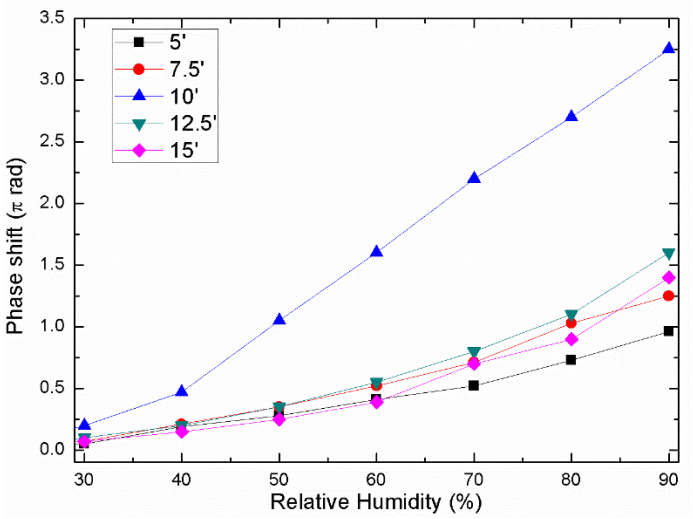

Fig. 8. Phase shift of sensors with different deposition times towards relative humidity.

After the sputtering deposition, a precise study of the results achieved inside the MOF cavity was carried out through the Optical Backscatter Reflectometer LUNA 4600. This device performs spatial measurements with resolution of 10 µm and allows the orthogonal polarizations states of light S and P to be analyzed. Fig.9 a) shows the Luna backscatter results for the MOF cavity before the sputtering deposition whereas Fig.9 b) represents the same MOF cavity after the deposition.

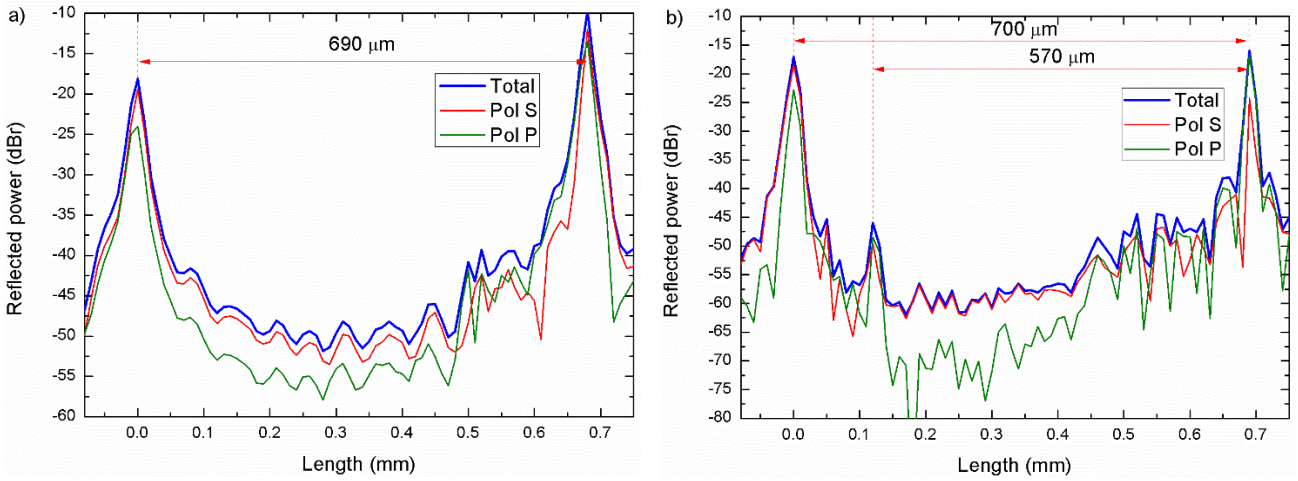

Fig. 9. Luna backscatter optical power of the MOF cavity and orthogonal polarization states: a) before sputtering deposition and b) after it.

Two main reflections are observable in Fig.9 a): the first one (set as reference) located at 0.0 mm corresponds to the splice between the SMF and the MOF fibers and it produces a light reflection of -17.6 dBr; the second relevant reflection is located at 0.690 mm and corresponds to the cleaved end of the MOF cavity giving a reflection power of -10 dBr. It must be also noticed that although there is a difference in the optical power reflected by the different polarization states: this difference is almost the same one along the whole MOF cavity (3.46 dB).

After the deposition, as Fig.9 b) illustrates, the splice location remains at the same point, but the cavity end is shifted 10µm. This length increase is due to the SnO_2 deposition on the second interface of the fiber cavity, although it is not a precise measurement because of the LUNA resolution limit; furthermore, a new reflection peak appears located at 0.130 mm. This new peak means that at this point, there is something affecting the light propagation along the core in the MOF cavity: the SnO_2 deposition depth limit. From this point towards the cleaved cavity end, the whole reflected light has changed. This effect is even easier to appreciate on the polarization states: polarization P is severely affected by the SnO_2 presence giving strong differences in relation to polarization S behavior. By measuring the distance from the cavity end to the new reflection point it can be assumed that the deposition depth inside the cavity is about 570 µm which means 130 µm before the cavity physical length limit. The SnO_2 deposition inside the MOF cavity in addition to the deposition on the top of the fiber ensure the interaction zone between the evanescent field of the guided light and the deposited thin film. As far as authors know it is the first time that an OBR is used in order to determine a sputtering thickness at the end of the fiber and it complements perfectly the results obtained from the SEM pictures' analysis. Moreover it is also the first time that an OBR is used to provide information of how a chemical deposition affects light inside a MOF.

2.6 Interrogation method

The interrogation technique is based on the Fast Fourier Transform of the sensor's optical spectrum. By monitoring the Fast Fourier Transform phase, wavelength shifts in the optical spectrum can be monitored without the noise influence or signal amplitude variations and enabling multiplexing several sensors within a single interrogator's channel as it will be

explained in section 3.4. Optical spectrum signal amplitude undesired variations lead to changes in the FFT module amplitude but do not affect the FFT phase.

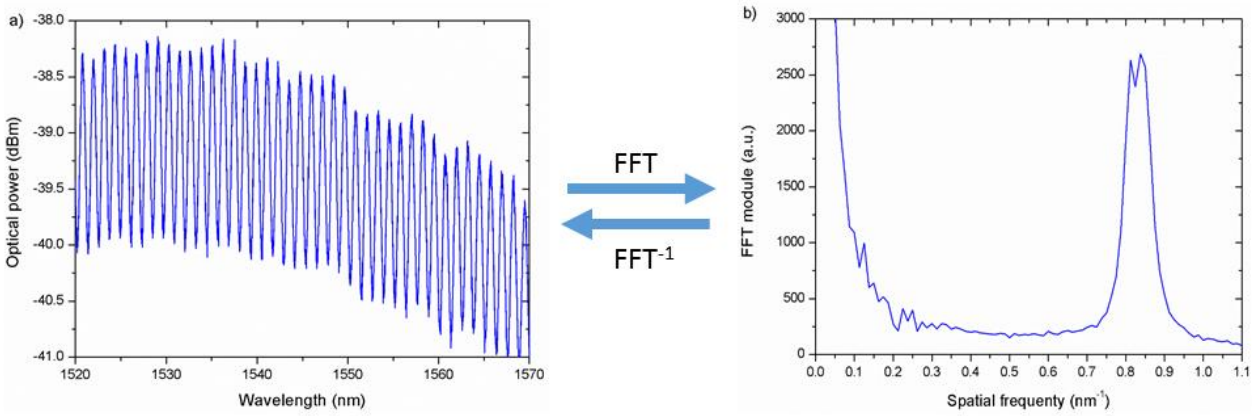

Fig. 10. Optical spectrum and its FFT.

A theoretically perfect periodical sinusoidal signal (such as the low finesse Fabry-Pérot response) in the optical spectrum domain presents two main components in the transformed domain (one in the positive part and its equivalent in the negative part) as can be seen in Fig. 10 (only positive part of the FFT module is shown). Real optical signals present some dispersion around the main transformed component due to the resolution of the optical interrogator but they can be assumed as a single contribution. Noise present in the optical spectrum is present in the transformed domain as high spatial frequency contributions and it can be neglected.

Wavelength shifts in the optical domain lead to phase shifts in the Fast Fourier Transform domain while the FFT module stays unaltered. By tracking the phase of the spatial frequency component (located in 0.8375 nm^{-1} in Fig. 10) the evolution of the optical spectrum and therefore the sensor can be monitored. Through this technique sensors can be monitored without the influence of signal amplitude noise or amplitude fluctuations and furthermore, it provides a useful multiplexing instrument.

3. Results and discussion

3.1 RH sensing

To verify the sensing head performance (and the influence of the SnO_2 deposition) with relative humidity variations, the fiber sensor was placed into the climatic chamber, and several experiments were implemented with RH variations from 20% to 90% at a constant 25ºC ±1 ºC temperature and at atmospheric pressure. The sensor response was measured tracking the FFT phase corresponding to spatial frequency located at 0.8375 nm^{-1}. Three increasing / decreasing relative humidity cycles were performed in each case to assure the time-stability of the sensor. Data were recorded using the Micron Optics SM 125 every 30 seconds and they were processed following the FFT algorithm. Furthermore, this device allows real time measurements to be recorded, although a sensor´s calibration is required. Fig. 11 presents the results of the MOF-FP cavity towards relative humidity cycles before and after SnO_2 deposition.

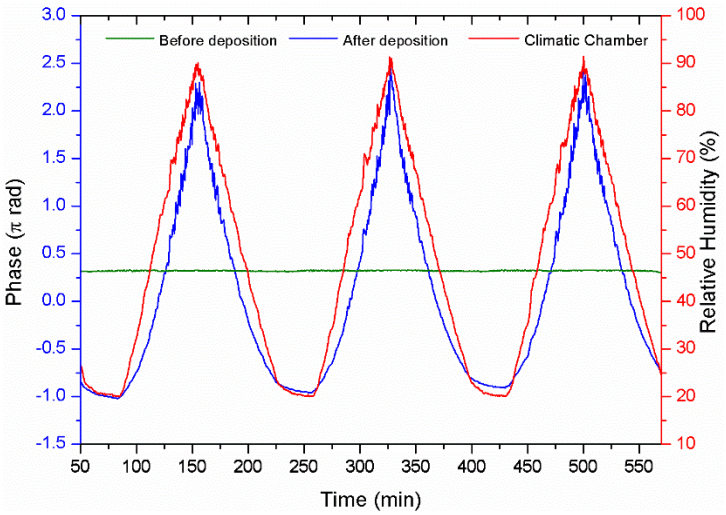

Fig. 11. Sensor's phase response: before deposition and after SnO_2 deposition.

On the one hand, as can be noticed from Fig. 11 (green line) the MOF cavity itself, without the SnO_2 layer presents negligible response to relative humidity variations. Direct guided light evanescent field interaction with the external medium do not show high variations giving a maximum shift of 0.015π rad from 20% to 90% RH. Furthermore, as it was previously commented, the high loss of the fiber and the low reflectivity of its core-air interface only allows a single round trip, which supposes a low capability to measure directly the surrounding medium.

On the other hand, Fig. 11(blue line) presents the MOF-FP-SnO_2 sensing head response after the sputtering deposition. It can be noticed that the sensitivity is improved, which sets maximum phase variation between 20% and 90% of 3.29π rad. Typically, the sensitivity of relative humidity sensors is different depending on the relative humidity range [18] showing 2-3 different regions with different sensitivities, but in our case, the sensor response shows a linear behavior in the whole measured relative humidity range with a constant sensitivity of 0.047π rad/% RH and a resolution of 0.0026% RH. In this manner, continous measures in the range 20%-90% RH can be performed without further callibrations. The sensor was tested repeatedly along two weeks to assure its repetibility, showing the same results in all cases.

3.2 Stability

One important feature of this type of sensors is its phase stability during time. To measure this parameter, the sensing head was placed in the climatic chamber at constant 40% RH and 25º C for 300 minutes and a sample was registered every minute. Fig. 12 shows the stability results with a maximum instability of 0.007 rad which implies an error of 5%.

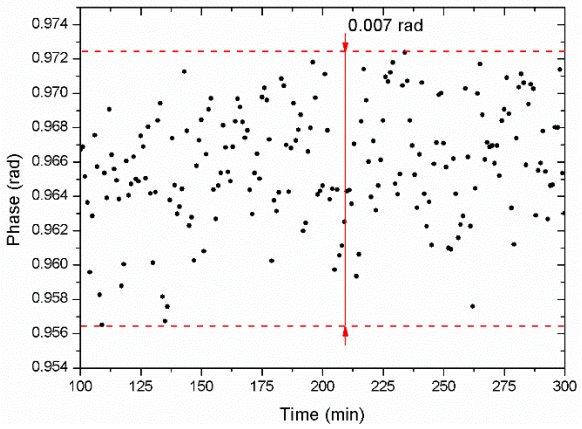

Fig. 12. MOF-FP-SnO_2 sensor's stability.

At this point, the influence of birefringence must be remarked. As the low-finesse Fabry-Pérot is highly birefringent, polarization affects its optical spectrum, showing important differences in the FFT module but slightly ones in the FFT phase. To reduce its influence, a polarizer and a stable optical bench were used during all the measurements.

3.3 Hysteresis

Another key feature in RH sensors is the hysteresis error. Usually metal oxide sensitive layers present low hysteresis effects in comparison with the polymeric ones [50] . In the MOF-FP-SnO_2 this tendency is also followed.

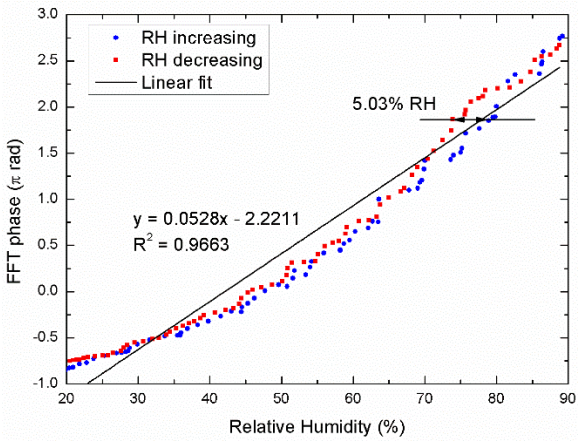

Fig. 13. Sensor's hysteresis.

The sensor presents low hysteresis with a maximum deviation of 5.03% RH showed in the high relative humidity region as Fig. 13 illustrates. This result agrees with the error produced due to the signal phase instability and can be influenced by it.

3.4 Multiplexing capability

As it was previously commented in section 2.2, the MOF cavity optical spectrum is directly influenced by its length (1). Varying appropriately the MOF length fused to the SMF it is possible to achieve different sensing heads with interferometric spectrums whose FFT modules do not overlap with each other. This way, if the main spatial component of each sensor in the FFT module is isolated, by tracking its FFT phase it is possible to measure independently avoiding crosstalk with the other sensors.

This FFT feature enables multiplexing high number of sensors within a single channel of the optical interrogator, reducing proportionally the economic cost of each sensor. Experimentally, authors have previously reported 3 multiplexed sensors [51] and successfully multiplexed up to 5 MOF-FP sensors with no crosstalk between measurements (work still not published) but theoretically it can be increased up to 10 without amplification needed. Furthermore, MOF-FP sensing heads with different sensitive layers can be multiplexed simultaneously increasing the versatility of the system becoming a multi-parameter and multi-point real-time monitoring system.

3.5 Temperature cross correlation

The influence of temperature variations on the MOF-FP-SnO_2 sensing head was experimentally tested. The performance of a MOF-FP cavity was previously tested by the authors [40] but not with the SnO_2 sensitive layer.

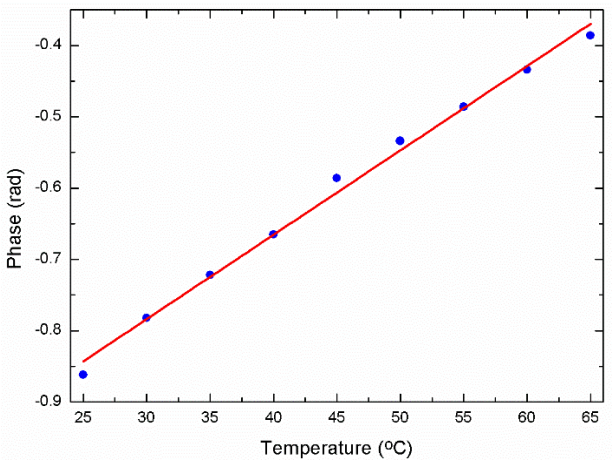

Fig. 14. MOF-FP-SnO_2 sensor's response to temperature.

As Fig.14 shows, the sensing head presents linear response to temperature variations with a sensitivity of 0.012 rad/ºC. This temperature influence is lower than the one reported from previous works [52] but it can produce crosstalk with RH measurements, although its effect can be compensated taking advantage of the system multiplexing capability: with a proper selection of MOF lengths, a MOF-FP-SnO_2 sensing head for RH measurements and a MOF-FP sensing head for temperature variations can be multiplexed. With the MOF-FP, temperature can be monitored independently of the RH and therefore it can be used as a reference for the others RH sensing head.

3.6 Breath measurements

In addition to the sensor sensitivity to RH variations, it presents two additional advantageous features: fast response and reversibility. These features make the MOF-FP-SnO_2 sensor suitable to be a real time human breath sensor. For this purpose, two different scenarios have been implemented with different devices and interrogating methods.

On the one hand the MOF-FP-SnO_2 sensing head was interrogated with a multi-LED source an analyzed in an OSA with a zero-spam method. Within this set up, the optical power temporal evolution at a certain wavelength of the optical spectrum was monitored. The OSA provides a sampling rate of 100 Hz with a maximum continuous measured period of 10 seconds and the results are shown in Fig. 15. The sensing head was placed close to the mouth of the target person and the RH variations produced by the exhalation were measured.

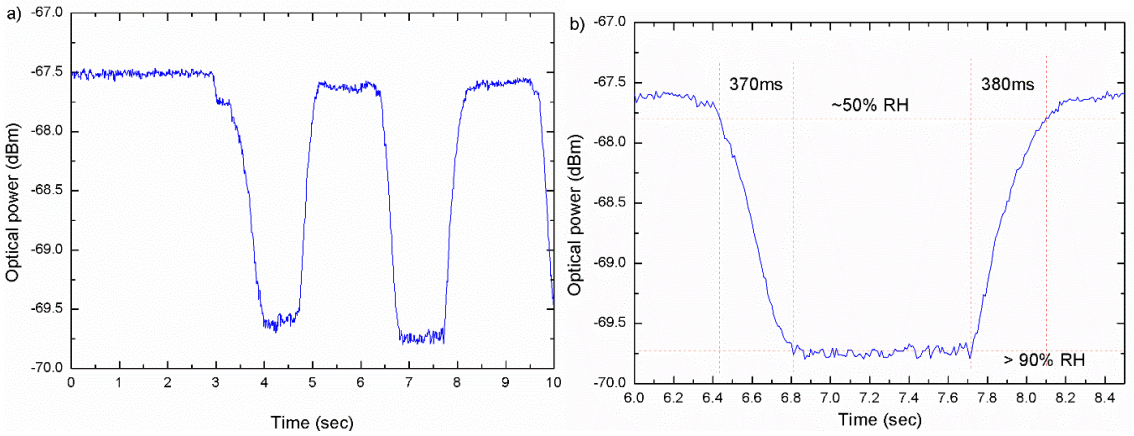

Fig. 15. a) Sensor's response to human breath using a zero span in the OSA and b) detail of one breath cycle.

The sensor responds continuously to human exhalation showing a response time of 370 ms, a recovery time of 380 ms: moreover, no baseline drift is observed.

On the other hand, additional measurements were performed with the optical interrogator Micron Optics si155 with a sample frequency of 10 Hz. With this device, RH can be tracked continuously and determined unambiguously in the whole range, as Fig. 16 illustrates.

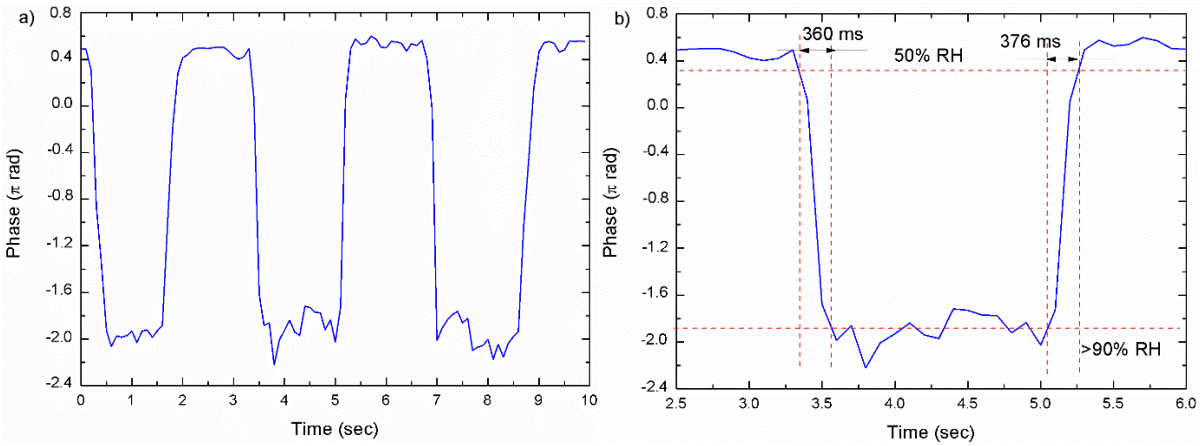

Fig. 16. a) Sensor's response to human breath using the si55 optical interrogator and b) detail of one breath cycle.

Once again, MOF-FP-SnO2 sensor shows similar rise and recovery time with full recovery of the baseline as it was expected. The difference between both interrogating methods lies on the capability of the second method (with the optical interrogator) to follow slow RH alterations during the exhalation period and the suitability of multiplexing several sensors at the same time. Furthermore, the recording and processing time of the system can be reduced using a high features computer.

4. Conclusions

A new sensor system for relative humidity measurements based on its interaction with a SnO_2 thin film sputtered on a MOF-Fabry-Pérot cavity has been proposed and experimentally demonstrated. The interrogation of the sensing head has been carried out through the FFT analysis. By monitoring the FFT phase variations of the low-finesse FP interference frequencies the optical spectrum can be tracked unambiguously. This method is low-dependent of the signal amplitude and avoids the necessity of tracking the wavelength evolution of maxima or minima of the spectrum, which can be a handicap when noise is present; it also allows several sensors to be multiplexed, which reduces the economic cost of the system and improves its versatility. The sensor has been operated within a wide relative humidity range (20%–90% RH), obtaining a maximum sensitivity achieved of 0.14 rad/% RH a resolution of 0.0026% RH and a phase standard deviation of 0.007 rad which presents an error of ±5%. Furthermore, FFT based signal processing makes the sensor response linear and along the entire RH range. The temperature influence can be real-time-compensated due to the multiplexing suitability of the interrogation technique. The SnO_2 MOF-FP sensor presents high-speed response, reversibility, high repeatability rate, robust and compact features. Furthermore, the baseline is always recovered without deviations, so that the device can be used for a real time applications such as breath monitoring.

Acknowledgments

The authors are grateful to A. Ortigosa, D. Erro, Dr. M. Bravo and Dr. R.A. Perez-Herrera. We also thank the Spanish Government projects TEC2013-47264-C2-2-R, TEC 2016-76021-C2-1-R, TEC2016-78047-R, TEC2016-79367-C2-2-R, Innocampus and the Cost Action MP 1401, as well as to the AEI/FEDER Funds.

References

[1] A. M. R. Pinto, M. Lopez-Amo, Photonic Crystal Fibers for Sensing Applications, Journal of Sensors, 21 (2012).
[2] T. M. Monro, S. Warren-Smith, E. P. Schartner, A. François, S. Heng, H. Ebendorff-Heidepriem, S. Afshar, Sensing with suspended-core optical fibers, Optical Fiber Technology, 16(6) (2010), 343-356.
[3] O. Frazao, J. L. Santos, F. M. Araújo, L. A. Ferreira, Optical sensing with photonic crystal fibers. Laser & Photonics Reviews, 2(6) (2008), 449-459.
[4] O. Frazao, S.F.O. Silva, J. Viegas, J.M. Baptista, J.L. Santos, J. Kobelke, K. Schuster, All Fiber Mach-Zehnder Interferometer Based on Suspended Twin-Core Fiber, IEEE Photonic Tech L 22 (2010), 1300-1302.
[5] A.S. Webb, F. Poletti, D.J. Richardson, J.K. Sahu, Suspended-core holey fiber for evanescent-field sensing, Opt Eng 46 (2007), 010503-010503-010503.
[6] M. Bravo, A. M. R. Pinto, M. Lopez-Amo, J. Kobelke, K. Schuster, High precision micro-displacement fiber sensor through a suspended-core Sagnac interferometer, Optics letters, 37(2) (2012), 202-204.
[7] S. Rota-Rodrigo, A. López-Aldaba, R. A. Pérez-Herrera, M. D. C. L. Bautista, Ó. Esteban, M. López-Amo, Simultaneous Measurement of Humidity and Vibration Based on a Microwire Sensor System Using Fast Fourier Transform Technique, Journal of Lightwave Technology, 34(19) (2016), 4525-4530.
[8] J. B. Jensen, L. H. Pedersen, P. E. Hoiby, L. B. Nielsen, T. P. Hansen, J. R. Folkenberg, J. Riishede, D. Noordegraaf, K. Nielsen, A. Carlsen, A. Bjarklev, Photonic crystal fiber based evanescent-wave sensor for detection of biomolecules in aqueous solutions. Optics letters, 29(17) (2004), 1974-1976.
[9] J. Bürck, J. P. Conzen, H. J. Ache, A fiber optic evanescent field absorption sensor for monitoring organic contaminants in water, Fresenius' journal of analytical chemistry, 342(4-5) (1992), 394-400.
[10] M. Tabib-Azar, B. Sutapun, R. Petrick, A. Kazemi, Highly sensitive hydrogen sensors using palladium coated fiber optics with exposed cores and evanescent field interactions, Sensors and actuators B: Chemical, 56(1) (1999), 158-163.
[11] S. Sekimoto, H. Nakagawa, S. Okazaki, K. Fukuda, S. Asakura, T. Shigemori, S. Takahashi, A fiber-optic evanescent-wave hydrogen gas sensor using palladium-supported tungsten oxide, Sensors and Actuators B: Chemical, 66(1) (2000), 142-145.
[12] A. S. Webb, F. Poletti, D. J. Richardson, J. K. Sahu, Suspended-core holey fiber for evanescent-field sensing, Optical Engineering, 46(1) (2007), 010503-010503.
[13] H. Choi, K. Park, S. Park, U. Paek, B. Lee, E. Choi, Miniature fiber-optic high temperature sensor based on a hybrid structured Fabry-Perot interferometer, Optics Letters (2008), 2455-2457.
[14] G. Z. Xiao, A. Adnet, Z. Zhang, F. G. Sun, C. P. Grover, Monitoring changes in the refractive index of gases by means of a fiber optic Fabry-Perot interferometer sensor, Sensors and Actuators A: Physical, 118(2) (2005), 177-182.
[15] L. H. Chen, T. Li, C. C. Chan, R. Menon, P. Balamurali, M. Shaillender, B. Neu, X.M. Ang, P. Zu, K. C. Leong, Chitosan based fiber-optic Fabry–Perot humidity sensor, Sensors and Actuators B: Chemical, 169 (2012), 167-172.
[16] O. Frazao, S. H. Aref, J. M. Baptista, J. L. Santos, H. Latifi, F. Farahi, J. Kobelke, K. Schuster, Fabry–Pérot cavity based on a suspended-core fiber for strain and temperature measurement, IEEE Photonics Technology Letters, 21(17) (2009), 1229-1231.
[17] M. J. Gander, W. N. MacPherson, J. S. Barton, R. L. Reuben, J. D. Jones, R. Stevens, K.S. Chana, S.J. Anderson, T. V. Jones, Embedded micromachined fiber-optic Fabry-Perot pressure sensors in aerodynamics applications, IEEE sensors Journal, 3(1) (2003), 102-107.
[18] J. Mathew, Y. Semenova, G. Rajan, G. Farrell, Humidity sensor based on photonic crystal fibre interferometer, Electronics Letters 43(19) (2010), 1341 – 1343.
[19] M. Hernaez, D. Lopez-Torres, C. Elosua, I.R. Matias, F.J. Arregui, Sensitivity Enhancement of a Humidity Sensor Based on poly (sodium phosphate) and poly (allylamine hydrochloride), Sensors 13(2012), 1930-0395.
[20] F.J. Arregui, Sensors Based on Nanostructured Materials, New York (NY): Springer, 2009.

[21] M. Stowell, J. Müller, M. Ruske, M. Lutz, T. Linz, RFsuperimposed DC and pulsed DC sputtering for deposition of transparent conductive oxides, Thin Solid Films (2007), 7654-7657.
[22] G. S. Devi, S. Manorama, V. J. Rao, High sensitivity and selectivity of an SnO2 sensor to H2S at around 100° C, Sensors and Actuators B: Chemical, 28(1) (1995), 31-37.
[23] R. N. Mariammal, K. Ramachandran, B. Renganathan, D. Sastikumar, On the enhancement of ethanol sensing by CuO modified SnO 2 nanoparticles using fiber-optic sensor, Sensors and Actuators B: Chemical, 169(2012), 199-207.
[24] H. E. Endres, W. Göttler, R. Hartinger, S. Drost, W. Hellmich, G. Müller, Ch.B. Braunmühl, A. Krenkow, C. Perego, G. Sberveglieri, A thin-film SnO2 sensor system for simultaneous detection of CO and NO2 with neural signal evaluation, Sensors and Actuators B: Chemical, 36(1-3) (1996), 353-357.
[25] J. Mizsei, Response pattern of SnO2 sensor system for smoke of different origins, Sensors and Actuators B: Chemical, 18(1-3) (1994), 264-267.
[26] J. Z. Ou, M. H. Yaacob, J. L. Campbell, M. Breedon, K. Kalantar-zadeh, W. Wlodarski, H 2 sensing performance of optical fiber coated with nano-platelet WO 3 film, Sensors and Actuators B: Chemical (2012), 166, 1-6.
[27] J. Dai, M. Yang, X. Yu, H. Lu, Optical hydrogen sensor based on etched fiber Bragg grating sputtered with Pd/Ag composite film, Optical Fiber Technology, 19(1) (2013), 26-30.
[28] N. Cennamo, D. Massarotti, L. Conte, L. Zeni, Low cost sensors based on SPR in a plastic optical fiber for biosensor implementation, Sensors, 11(12) (2011), 11752-11760.
[29] C. Bariain, I. R. Matías, F. J. Arregui, M. Lopez-Amo, Experimental results towards development of humidity sensors by using a hygroscopic material on biconically tapered optical fibre, Proceedings of SPIE, 3555, (1998), 95-105.
[30] S. Akita, H. Sasaki, K. Watanabe, A. Seki, A humidity sensor based on a hetero-core optical fiber, Sensors and Actuators B: Chemical, 147(2) (2010), 385-391.
[31] F. J. Arregui, Y. Liu, I. R. Matias, R. O. Claus, Optical fiber humidity sensor using a nano Fabry–Perot cavity formed by the ionic self-assembly method, Sensors and Actuators B: Chemical, 59(1) (1999), 54-59.
[32] M. Konstantaki, S. Pissadakis, S. Pispas, N. Madamopoulos, N. A. Vainos, Optical fiber long-period grating humidity sensor with poly (ethylene oxide)/cobalt chloride coating, Applied optics, 45(19) (2006), 4567-4571.
[33] P. Kronenberg, P. K. Rastogi, P. Giaccari, H. G. Limberger, Relative humidity sensor with optical fiber Bragg gratings, Optics letters, 27(16) (2002), 1385-1387.
[34] F. C. Favero, J. Villatoro, V. Pruneri, Microstructured optical fiber interferometric breathing sensor, Journal of biomedical optics, 17(3) (2012), 0370061-0370065.
[35] J. Witt, F. Narbonneau, M. Schukar, K. Krebber, J. De Jonckheere, M. Jeanne, D. Kinet, B. Paquet, A. Depré, L.T. DÁngelo, T. Thiel, R. Logier, Medical textiles with embedded fiber optic sensors for monitoring of respiratory movement. IEEE sensors journal, 12(1) (2012), 246-254.
[36] A. Grillet, D. Kinet, J. Witt, M. Schukar, K. Krebber, F. Pirotte, A. Depré, Optical fiber sensors embedded into medical textiles for healthcare monitoring, IEEE Sensors Journal, 8(7) (2008), 1215-1222.
[37] Y. Kang, H. Ruan, Y. Wang, F. J. Arregui, I. R. Matias, R. O. Claus, Nanostructured optical fibre sensors for breathing airflow monitoring, Measurement Science and Technology, 17(5) (2006), 1207.
[38] S. Muto, O. Suzuki, T. Amano, M. Morisawa, A plastic optical fibre sensor for real-time humidity monitoring, Measurement Science and Technology, 14(6) (2003), 746.
[39] A. Lopez-Aldaba, D. Lopez-Torres, J. Ascorbe, S. Rota-Rodrigo, C. Elosua, M. Lopez-Amo, F.J. Arregui, J.M. Corres, J.-L. Auguste, R. Jamier, P. Roy, SnO2-MOF-Fabry-Pérot humidity optical sensor system based on fast Fourier transform technique, Sixth European Workshop on Optical Fibre Sensors (pp. 99161T-99161T) (2016), International Society for Optics and Photonics.
[40] A. Lopez-Aldaba, A.M.R. Pinto, M. Lopez-Amo, O. Frazão, J.L. Santos, J.M. Baptista, H. Baierl, J.L. Auguste, R. Jamier, P. Roy, Experimental and Numerical Characterization of a Hybrid Fabry-Pérot Cavity for Temperature Sensing, Sensors 15 (2015), 8042-8053.
[41] B. D. Gupta, C. D. Singh, Fiber-optic evanescent field absorption sensor: A theoretical evaluation, Fiber & Integrated Optics, 13(4) (1994), 433-443.
[42] S. K. Khijwania, B. D. Gupta, Fiber optic evanescent field absorption sensor: effect of fiber parameters and geometry of the probe, Optical and Quantum Electronics, 31(8) (1999), 625-636.
[43] J. L. Santos, A. P. Leite, D. A. Jackson, Optical fiber sensing with a low-finesse Fabry–Perot cavity, Applied optics, 31(34) (1992), 7361-7366.

[44] D. Leandro, M. Bravo, A. Ortigosa M. Lopez-Amo, Real-time FFT analysis for interferometric sensors multiplexing, J Lightwave Technol. 33(2) (2015), 354-360.
[45] J. Ascorbe, J. M. Corres, I. R. Matias, F. J. Arregui, High sensitivity humidity sensor based on cladding-etched optical fiber and lossy mode resonances, Sensors and Actuators B: Chemical, 233 (2016), 7-16.
[46] J. Ascorbe, J. M. Corres, F. J. Arregui, I. R. Matias, Humidity Sensor Based on Bragg Gratings Developed on the End Facet of an Optical Fiber by Sputtering of One Single Material, Sensors, 17(5) (2017), 991.
[47] W. Schmid, Consumption measurements on SnO2 sensors in low and normal oxygen concentration (Doctoral dissertation, Universität Tübingen), (2004).
[48] D. Lopez-Torres, C. Elosua, J. Villatoro, J. Zubia, M. Rothhardt, K. Schuster, F. J. Arregui, Photonic crystal fiber interferometer coated with a PAH/PAA nanolayer as humidity sensor, Sensors and Actuators B: Chemical, 242 (2017), 1065-1072.
[49] D. Lopez-Torres, C. Elosua, J. Villatoro, J. Zubia, M. Rothhardt, K. Schuster F.J. Arregui, Enhancing sensitivity of photonic crystal fiber interferometric humidity sensor by the thickness of SnO2 thin films, (2017), Sensors and Actuators B: Chemical.
[50] C. Massaroni, M. A., Caponero, R. D'Amato, D. Lo Presti, E. Schena, Fiber Bragg Grating Measuring System for Simultaneous Monitoring of Temperature and Humidity in Mechanical Ventilation. Sensors (2017), 17(4), 749.
[51] A. Lopez-Aldaba, D. Lopez-Torres, C. Elosua, J.-L. Auguste, R. Jamier P. Roy, F.J. Arregui, M. Lopez-Amo, Relative humidity multi-point optical sensors system based on fast Fourier multiplexing technique. In 25th International Conference on Optical Fiber Sensors (pp. 103233L-103233L) (2017, April). International Society for Optics and Photonics.
[52] J. Mathew, Y. Semenova, G. Farrell, Experimental demonstration of a high-sensitivity humidity sensor based on an Agarose-coated transmission-type photonic crystal fiber interferometer, Applied optics, 52(16) (2013), 3884-3890.

Author Biographies

Aitor Lopez-Aldaba: was born in Navarra, Spain, in July 1988. He received the, Telecommunication Engineering degree from the Universidad Pública de Navarra, Navarra, in 2014. In 2013, he joined the Optical Communications Group, Department of Electrical and Electronic Engineering, Universidad Pública de Navarra. His research interests include fiber optic lasers, optical amplifiers, optical fiber sensor networks, photonic crystal fibers and chemical fiber optic sensors.

Diego López-Torres: received the M.S. degree in electrical and electronic engineering and the master's degree in communications from the Public University of Navarra (UPNA), Pamplona, Spain, in 2013 and 2014, respectively. Since 2014, he has been working as a Researcher at the UPNA. In 2105, he obtained a scholarship from this university. His research interest includes optical fiber sensors, photonic crystal fiber and nanostructured materials.

Cesar Elosúa Aguado: received his MS degree in electrical and electronic engineering from the Public University of Navarre (UPNA, Pamplona, Spain) in 2004. In the same year, he obtained a scholarship from the Science and Technology Spanish Ministry and he joined the optical fiber sensor group at UPNA. During 2008, he was a visiting Ph.D. student at the University of Limerick and at the City University of London. He became a lecturer of this department in 2009, receiving his PhD degree in the next year. His research interests include optical fiber sensors and networks, organometallic chemistry and data mining techniques.

Raphael Jamier: was born in Périgueux, France, in 1981. He received the Ph.D. degree in 2007 from the University of Limoges, France. Since 2008, he has been an Assistant professor at XLIM research institute / University of Limoges, where he has been engaged in design, fabrication and characterisation of specialty optical fibers. His current research activities include the design, fabrication and characterization of photonic crystal fibers for high-power generation at unconventional spectral domains (in particular in the mid-infrared wavelengths). He is also the Deputy Director of the Physics Department of the University of Limoges since 2012. - He has 27 articles as co-author/author in refereed journals, 58 papers in internationally recognized conferences with peer-review system and 2 patents.

Jean-Louis Auguste: received a PhD degree in Optical and High Frequency of Telecommunications from the University of Limoges (France) in 2001. During his thesis, the main areas of activity have been involved theory, design and experimental investigation on optical fibres and more particularly on a design and fabrication of high negative chromatic dispersion fibre. Since December 2000, he is a CNRS Engineer at Xlim research institute where he was, until 2012, in charge (Process Manager) of the research and development around fabrication of optical fibres – guide structure (PCF) and materials for optical fibres with recent developments around glass synthesis thanks to a European project (VORTEX) that he manages. He works in strong collaboration with researchers of the Fibre Group and is associated to ANR and other European Projects like researcher from Ceramic Laboratory to develop new topics mixing optical glass development and optical fibre applications. By this way in collaboration with researcher from SPCTS (Ceramic Laboratory) he manages a new research project at Xlim around 'original glasses for optical fibre applications'. He has authored or co-authored 45 publications in international journals with referees and 43 papers in international conferences with referees including several invited papers and international seminars plus 4 patent applications. In 2010, he has obtained the degree of HDR, highest diploma of University and giving him the possibility to

be Research Director for PhD students. A part of his activity is dedicated to teaching and training students from University and school engineering.

Francisco J.Arregui: (M'01) is a Full Professor at the Public University of Navarre, Pamplona, Spain. He was part of the team that fabricated the first optical fiber sensor by means of the Layer-by-Layer assembly method at Virginia Tech, Blacksburg, VA, USA, in 1998. He is the author of around 300 scientific journal and conference publications. He has been an Associate Editor of "IEEE Sensors Journal", "Journal of Sensors" (founded by Prof, Arregui in 2007), and "International Journal on Smart Sensing and Intelligent Systems". He is also the editor of the books entitled Sensors- Based on Nanostructured Materials and Optochemical Nanosensors.

Philippe Roy: was born in May 1971 in Bellac (France) and received his Ph Degree in Microwave Electronics and Optoelectronics (speciality Photonics and Electronics Systems) in 1997 in the University of Limoges. He is now a CNRS senior researcher and head of Fibre Photonics group at XLIM, which is a mixed laboratory of University of LIMOGES and CNRS. Since 1998, he is involved in design, fabrication and characterisation of Photonic Crystal fibres (PCFs). More recently, he developed specialty and composite fibres mainly dedicated to advanced fibre sensor systems and to very high power fibre lasers. He develops rare earth doped fibre with complex structure based on an aperiodic design to reach higher power levels without modal instabilities and/or non-conventional emitted spectrum, from visible to THz domain.

Manuel López-Amo (M'91–SM'98) was born in Madrid, Spain, in 1960. He received the Telecommunications Engineering and Ph.D. degrees from the Universidad Politécnica de Madrid, Madrid, in 1985 and 1989, respectively. From 1985 to 1996, he belonged to the Photonic Technology Department, Universidad Politécnica de Madrid, where, in 1990, he became an Associate Professor. In 1996, he moved to the Electrical and Electronic Engineering Department, Public University of Navarra, Pamplona, Spain, where he became a Full Professor and is currently the Head of the Optical Communications Group. He has been the Chairman of the Optoelectronic Committee of Spain. He has been the leader of more than 40 research projects and he has coauthored more than 250 works in international refereed journals and conferences related with fiber-optic networks, optical amplifiers, fiber-optic sensors, and integrated optics. He is a member of the technical committees of the International Conference on Fiber Optic Sensors and the European Workshop on Optical Fiber Sensors, among others. He is a senior member of the IEEE and member of the Optical Society of America.